Biol. Cybernetics 27, 199—213 (1977)

Biological Cybernetics

A Point Process Analysis of the Spontaneous Activity of Anterior Semicircular Canal Units in the Anesthetized Pigeon*

M. J. Correia

Departments of Otolaryngology, Physiology and Biophysics, Galveston, Texas, USA

J. P. Landolt

Defence and Civil Institute of Environmental Medicine, Downsview, Ontario, Canada

Abstract. A point process analysis was performed on extracellular trains of spontaneous activity, which were recorded from anterior semicircular canal units in Scarpa's ganglion in the anesthetized pigeon. For stationary units, the mean interspike interval (ISI) varied from 4.00 to 51.22 ms, and the coefficient of variation ranged from 0.05 to 0.88. Selected tests indicated that 63.6% of units had the properties of a renewal process. The ISI histograms of these "renewal"-type units were fitted with several probability density functions (pdfs) including the gamma, exponential, exponential-with-delay and the pdf for the first passage times (fpts) in a Wiener-Lévy (WL) process. The WL process provided a good fit to "irregular" discharge patterns. Furthermore, a neurophysiological basis for this process exists within the vestibular neuroepithelium. It is conjectured that a generalization of this process would also describe "regular" discharge patterns which have been observed in the spontaneous activity of vestibular primary afferents.

Introduction

Wersäll (1956) first demonstrated that the vestibular neuroepithelium consists of two kinds of hair cells. The Type I hair cell, which is only found in the mammal, bird and reptile, is bottle-shaped and is innervated by a nerve fiber whose calycine ending forms a shell around the cell. The Type II hair cell is cylindrical and is innervated by two or more bouton-type endings possibly from several nerve fibers. Other recent ultrastructural observations show that the innervation of the vestibular neuroepithelia is, indeed, complex; e.g., there is not a one to one correspondence between each hair cell and a primary afferent fiber. In fact, a single nerve fiber may make contact with several hair cells; and, often, an individual hair cell is innervated by several nerve fibers (Iurato and Taidelli, 1964; Smith and Rasmussen, 1968; Engström et al., 1972; Jørgensen and Andersen, 1973).

It is very difficult to record the intracellular potentials directly from these hair cells with any degree of reliability or consistency. In the first place, these cells are small [20–40 μm in length and 4–10 μm in diameter (Flock, 1971)]. Secondly, the hair cells of the vestibular and auditory organs are enclosed within the membranous and bony labyrinths in the skull and any approach to either of these cells necessarily destroys the integrity of the entire system. Thirdly, any technique which exposes the hair cells for recording purposes unavoidably interferes with the equilibrium of the otic fluids bathing them and may also jeopardize their vascular supply. Any such interruptions of the normal otic metabolism may cause changes in the intracellular potentials of the hair cells.

Many of these problems can be overcome or minimized by recording extracellularly the spike train activity from the primary afferents which make synaptic contact with the hair cells. Data from other neural structures (Junge and Moore, 1966; Calvin and Stevens, 1968) show that the membrane potential fluctuations recorded intracellularly do correlate well with the variability in the interspike intervals (ISIs) associated with the extracellular recording of spike train data.

In previous studies, the spontaneous discharge patterns from primary afferents of the cristae ampullares were characterized simply by their first-order statistical properties (Goldberg and Fernandez, 1971; Correia and Landolt, 1973; Lifschitz, 1973). This procedure is insufficient to model the process which generates and characterizes vestibular primary afferent discharges. In this paper, we have applied a set of more stringent tests (Lewis et al., 1969; Landolt and Correia, 1977) to determine whether or not selected units can be

* DCIEM Research Paper 76-X-58

characterized by the first-and second-order properties of their discharge patterns. In those units which passed these tests and qualified as being from a renewal process, we attempted to specify their first-order properties more precisely by fitting several probability density functions (pdfs) to their ISI histograms. Additionally, we applied second-order analytical techniques to all units to elicit further information. Finally, we have used our results, combined with neuroanatomical and neurophysiological observations, to make significant inferences about the generation of spontaneous activity in the vestibular sensory neuroepithelia.

Methods

Experimental

White King pigeons *(Columba livia)* were used as experimental animals. Trains of spontaneous activity were recorded with metal microelectrodes from 120 primary afferent neural units which innervated the crista ampullaris of the right anterior semicircular duct. Data acquisition was begun after allowing 2 min stabilization with the bird's sagittal head plane perpendicular to an earth-fixed vertical. Spike activity was processed by means of a Model 1074 physiological signal analyzer (Nicolet Instrument Corp.) and stored on DECtape (Digital Equipment Corp.) for further analysis. The ISIs were determined with a resolution of 1.0 ms. These intervals and the ISI histograms which were formed from them constitute the data base for the analysis presented herein.

Prior to the recording session, each bird was anesthetized by I.V. injection of approximately 1.0 ml Equi-Thesin® and subsequent doses of 0.2 ml were administered as necessary. Equi-Thesin® consists of chloral hydrate (42.50 mg/ml), pentobarbital (9.72 mg/ml) and magnesium sulfate (21.26 mg/ml) in 42.8% propylene glycol, 11.5% alcohol and distilled water. Other techniques used in surgery, microelectrode fabrication, single unit isolation, and data acquisition have been outlined in more detail elsewhere (Correia et al., 1973).

Computational

The ISIs for all 120 units were initially screened by performing a test of stationarity using a PDP/9T computer (Digital Equipment Corp.). This test, the Wald-Wolfowitz runs test (Himmelblau, 1970), was applied to different segments of the sample spike train which included: 1. the entire spike train 0-L (L = total number of spikes in the sample, which varied from 3427 to 4095 spikes) subdivided into 128 time interval lengths (TILs); 2. the record length from 0-2048 spikes subdivided into 64 TILs; and 3. the record lengths 0-1024, 1025-2048, 2049-3072, and 3073-L, each of which was subdivided into 32 TILs. Except for the record length 3073-L, the mean number of spikes per TIL varied from 27 to 32 spikes; values considered to represent a compromise between larger numbers which might mask out any trends due to too lengthy a segment, and smaller ones which would not give enough variation for a justifiable statistical analysis. Departures from stationarity were tested using the approximate standard normal variate, $Z=(|r-\hat{\mu}_r|-\frac{1}{2})/SD_r$, where $r \equiv$ number of runs, and $\hat{\mu}_r$ and SD_r are the mean and standard deviation of r, respectively.

For units whose ISI data were determined to be stationary by the Wald-Wolfowitz runs test, estimates of the mean interval, $\hat{\mu}_x = (1/n)\sum_{i=1}^{n} x_i$; variance, $\hat{\sigma}_x^2 = m_2$; standard deviation, $SD=(m_2)^{1/2}$; mean firing rate, $\lambda = 1/\hat{\mu}_x$; coefficient of variation, $CV = SD/\hat{\mu}_x$; coefficient of skewness, $\hat{\beta}_1 = m_3^2/m_2^3$; coefficient of kurtosis, $\hat{\beta}_2 = m_4/m_2^2$; and coefficient of excess, $(\hat{\beta}_2 - 3)$, were determined. In the above equations, $m_k = (1/n)\sum(x_i - \hat{\mu}_x)^k$ $(k = 2, 3, 4, \ldots)$.

Based upon the results of the stationarity test and the characterization of the spike train data by their first-order properties, ISI samples ($n = 1024$) from 22 representative units were analyzed as a point process by means of a computer program, SASE IV (Lewis et al., 1969) with a PDP/10 computer (Digital Equipment Corp.). (A larger sample would have been prohibitive because of the large amount of computation time required to study each unit.) In order to assess the accuracy and efficiency of SASE IV, the computer programs which comprise this package were used to analyze an artificial Poisson process (APP). The APP was produced by first generating a series of uniformly-distributed, random numbers $u(0, 1)$ with the PDP/10 computer (mean value, $\mu_x = 10$) and then calculating a series of random numbers, $-\log_e u(0, 1)$. These values represent a sample drawn from an exponential distribution with parameter 1.0, and therefore represent the duration between successive events of a Poisson process having unit mean rate.

Tests of independence of intervals were performed using statistics based on serial correlation coefficients, the spectral density of intervals and exponentially-ordered scores. SASE IV was used to obtain estimates of the serial correlation coefficients

$$\hat{\varrho}_j = \frac{n}{(n-1)(n-j)} \frac{1}{\hat{\sigma}_x^2} \sum_{i=1}^{n-j} (x_i - \hat{\mu}_x)(x_{i+j} - \hat{\mu}_x)$$

$$(j = 1, \ldots, n), \tag{1}$$

whose test statistic, $\hat{\varrho}_j (n-j)^{1/2}$, represents a standard normal variate for large values; the spectral density function of the time intervals

$$\hat{f}_+(\omega) = \frac{1}{\pi}\left[1 + 2\sum_{j=1}^{\infty} \hat{\varrho}_j \zeta_j \cos(j\omega)\right] \quad (0 \leqq \omega \leqq \pi), \tag{2}$$

where ζ_j represents a Parzen weighting sequence (Cox and Lewis, 1966) whose values were suitably chosen as a compromise between smoothing and resolution of detail in $\hat{f}_+(\omega)$; and exponentially-ordered scores,

$$E_n(j) = \sum_{i=1}^{j} 1/(n-i+1) \quad (j = 1, \ldots, n), \tag{3}$$

which represent the expected value of the j^{th} largest interval of $\{x_i\}$ from a unit exponential distribution of size n. When each of the original sequentially-ordered x_i's is replaced by its corresponding $E_n(j)$ and a new series, with set $\{z_i\}$, is formed, the following product-moment test statistic can be calculated

$$\hat{R}_h = \sum_{i=1}^{n-h} z_i z_{i+h}. \tag{4}$$

The distribution of R_h for three lags ($h = 1, 2, and\ 3$) under the null hypothesis of independence has been tabulated by Lewis and Goodman (1968).

In addition to the general tests of stationarity and independence described above, the data were tested against the following point processes:

a. Time-Dependent Poisson Process. The test is for a trend (non-stationarity) in the rate of occurrence, $\lambda(x)$, of a time-dependent Poisson process. The form

$$\lambda(x) = e^{\alpha + \beta x} \tag{5}$$

is used and the test is for $\beta = 0$ versus $\beta \neq 0$ (α is only a scale factor) using a statistic (hereafter called V-statistic) derived by Cox and Lewis (1966, pp. 45–51). This statistic has a standardized normal form for large n.

b. Standard Poisson Process. For a Poisson process, the quantities

$$Y_i = s_i/s_n \quad (i=1,2,\ldots,n) \tag{6}$$

represent the order statistics from a random sample of size n which is uniformly distributed $u(0,1)$. In (6), s_i and s_n are the total time lengths to the i^{th} and n^{th} spike, respectively. Similarly, by ordering the intervals between events in increasing magnitude, x_i^1, the quantities

$$W_i = \{x_1^1 + x_2^1 + \ldots + x_{i-1}^1 + (n+2-i)x_i^1\}/s_n \tag{7}$$

also have the same distributional properties as the Y_i's for the null Poisson hypothesis. Equation (7) is used to gain power against certain false null hypotheses for which the power of the goodness-of-fit test of the Y_i's is low. Goodness-of-fit of the distributions of Y_i and W_i was tested using the distribution-free, one-sided Kolmogorov-Smirnov and Anderson-Darling statistics; the asymptotic significance values of which are tabulated on p. 258 in Cox and Lewis (1966). [For $CV < 1.0$, we used a one-sided form of the Kolmogorov-Smirnov statistic (cf. Lewis, 1965).]

c. Ordinary Renewal Process. Specific tests of the null hypothesis for a renewal process are based on the argument (Bartlett, 1954) that the estimates of its periodogram have asymptotically independent and identical exponential distributions with mean value, $1/\lambda = \hat{\sigma}_x^2/\pi$. The alternative hypothesis is for a non-constant spectrum. The periodogram is defined as $c_j = |a_j|^2/2\pi n\sigma_x^2$, where the a_j's are complex numbers that have been determined by the finite Fourier transform of the intervals, x_i. The quantities

$$C_j = \left(\sum_{i=1}^{j} c_i\right) \Big/ \left(\sum_{i=1}^{n/2-1} c_i\right) \quad \left(j=1,\ldots,\frac{n}{2}-1\right) \tag{8}$$

should, thus, represent the order statistics from a uniform distribution $u(0,1)$. The Anderson-Darling and one-sided Kolmogorov-Smirnov statistics were used to estimate the uniformity of the C_j's.

d. Renewal Process in which ISIs *are Distributed According to a Gamma Distribution Function.* We used the Moran statistic (Lewis, 1965),

$$M = -2\sum_{i=1}^{n} \log_e(x_i/\hat{\mu}_x), \tag{9}$$

to test the Poisson hypothesis against the alternative renewal process having ISIs distributed in the form of a gamma pdf, i.e.,

$$p(x) = \lambda^\delta x^{\delta-1} e^{-\lambda x}/\Gamma(\delta) \quad (\delta \geqq 0, 0 \leqq x \leqq \infty), \tag{10}$$

where $\Gamma(\delta)$ is the Gamma function and δ is a shape parameter. For $\delta = 1$, $p(x)$ is exponential. We tested $\delta = 1$ against $\delta > 1$ with the Moran statistic, which has a χ^2-distribution with $n-1$ degrees of freedom (df) for large n.

In addition to tests relating to the *interval* aspects of a point process *(vide supra)*, we also evaluated the neural data using functions related to three second-order properties of the *counting* aspects of the process (see Cox and Lewis, 1966; Landolt and Correia, 1977, for a discussion of the differences between these two aspects). These three functions are the expectation density, $g(x)$, the variance-time curve, $Var[t]$, and the spectral density of the counting process, $I_+(\omega)$.

Formally, we may write

$$g(x) = \lim_{\Delta x \to 0^+} \frac{\text{prob}[\text{event in } (x, x+\Delta x) \,|\, \text{event at } x=0]}{\Delta x} \tag{11}$$

for the expectation density. We used a smoothed estimate of $g(x)$; namely,

$$\hat{g}(k\gamma + \gamma/2) = r_k s_n/[n\gamma(s_n - k\gamma - \gamma/2)], \tag{12}$$

where γ is the smallest interval over which "smoothing" occurs, and r_k represents the contribution of all possible sums of contiguous times between impulses in the spike train during successive intervals $k\gamma (k=1,2,\ldots)$. With the null hypothesis of a Poisson process, the approximate 5% confidence limits for an individual $\hat{g}(k\gamma+\gamma/2)$ are

$$[(n-1)/s_n] \pm 1.96/[\gamma(s_n - k\gamma - \gamma/2)]^{1/2}. \tag{13}$$

$Var[t]$ determines the way in which the variance of the number of impulses in a fixed interval of time, s_n, varies as a function of the time. Two methods were used to estimate $Var[t]$, both of which can be found in the literature [see p. 115–118 in Cox and Lewis (1966), and the description of the VART and COV subroutines in SASE IV (Lewis et al., 1969)]. To indicate the variance of the estimate $\hat{Var}[t]$ for a Poisson process, the expression

$$Var[\hat{Var}[t]] \simeq \frac{2n^2t^3}{3s_n^3} + \frac{4\Delta n^2 t^2}{3s_n^3} + \frac{nt^2}{s_n^2} \tag{14}$$

was used (Δ represents a binning interval over which impulse counting takes place).

The spectral density function, $I_+(\omega)$, converts a differential counting process from a time domain function to one in the frequency domain by means of a Fourier integral [Eq. (15), p. 74 in Cox and Lewis (1966)]. The actual form of the estimate $\hat{I}_+(\omega)$ that is used in SASE IV is quite cumbersome and can be located elsewhere (see p. 23 in Lewis et al., 1969). It should be noted, however, that the computer program estimates a normalized spectrum, $\hat{I}(\ell') = 2\pi s_n \hat{I}_+(\omega)/n$, which has the constant value 2.0 for the special case of a Poisson process. SASE IV uses a uniform weighting scheme to smooth the spectrum; the purpose of which is to obtain a consistent estimate of $I_+(\omega)$. Herein, the significance bands $(\chi^2_{2c,\alpha/2})/c$ and $(\chi^2_{2c,1-\alpha/2})/c$ were estimated for the spectrum when smoothed over successive sets of $c = 20\hat{I}_+(\omega)$ under the null hypothesis of a Poisson process. Thus, the probabilities that all points fall within these two bands are 0.95 at a level $\alpha = 0.001$ and 0.60 at $\alpha = 0.01$, respectively.

Curve-fitting techniques were applied to the ISI histogram data in order to determine a "best-fitting" pdf, $p(x)$, for representative units demonstrating the properties of a renewal process. The distributions which were chosen as possible fits to the ISI histograms all have a *potential* neurobiological basis for spike initiation in the vestibular neuroepithelium (see Discussion). These include the exponential, the exponential-with-delay, the gamma, and that for the first passage times (fpts) of a Wiener-Lévy (WL) process with absorbing barrier [pp. 219–223 in Cox and Miller (1965)]. The WL fpt pdf may be written as

$$p(x) = \frac{\theta_1}{\sqrt{2\pi x^3}} \exp\left[-\frac{(\theta_1)^2}{2x} - \frac{(\theta_2)^2 x}{2} + \theta_1\theta_2\right], \tag{15}$$

from which are obtained $\mu_x = \theta_1/\theta_2$, and $CV = (\theta_1\theta_2)^{-1/2}$.

These pdfs were fitted iteratively by a nonlinear curve-fitting program (Brassard et al., 1975) to the ISI histogram data by means of a PDP-11/20 minicomputer (Digital Equipment Corp.). The best fit parameters are indicated by the Least Squares Error (LSE), which is formed from the sum of the squared differences between each value of the best fit, candidate pdf and each corresponding value of the empirical ISI frequency distribution. We used the RMSE, which is defined as

$$\text{RMSE} = [\text{LSE}/(N-k)]^{1/2}, \tag{16}$$

to compare the goodness-of-fit of the derived pdf to that of the empirical data [$N \equiv$ number of class intervals (bins) in the histogram, and $k \equiv$ number of parameters]. The suitability of a candidate pdf as a model for an ISI histogram was determined by the distribution-free Kolmogorov-Smirnov (KS) statistic, D_n (Feller, 1948). We use P_{KS} (Table 2), which is the probability associated with the limiting

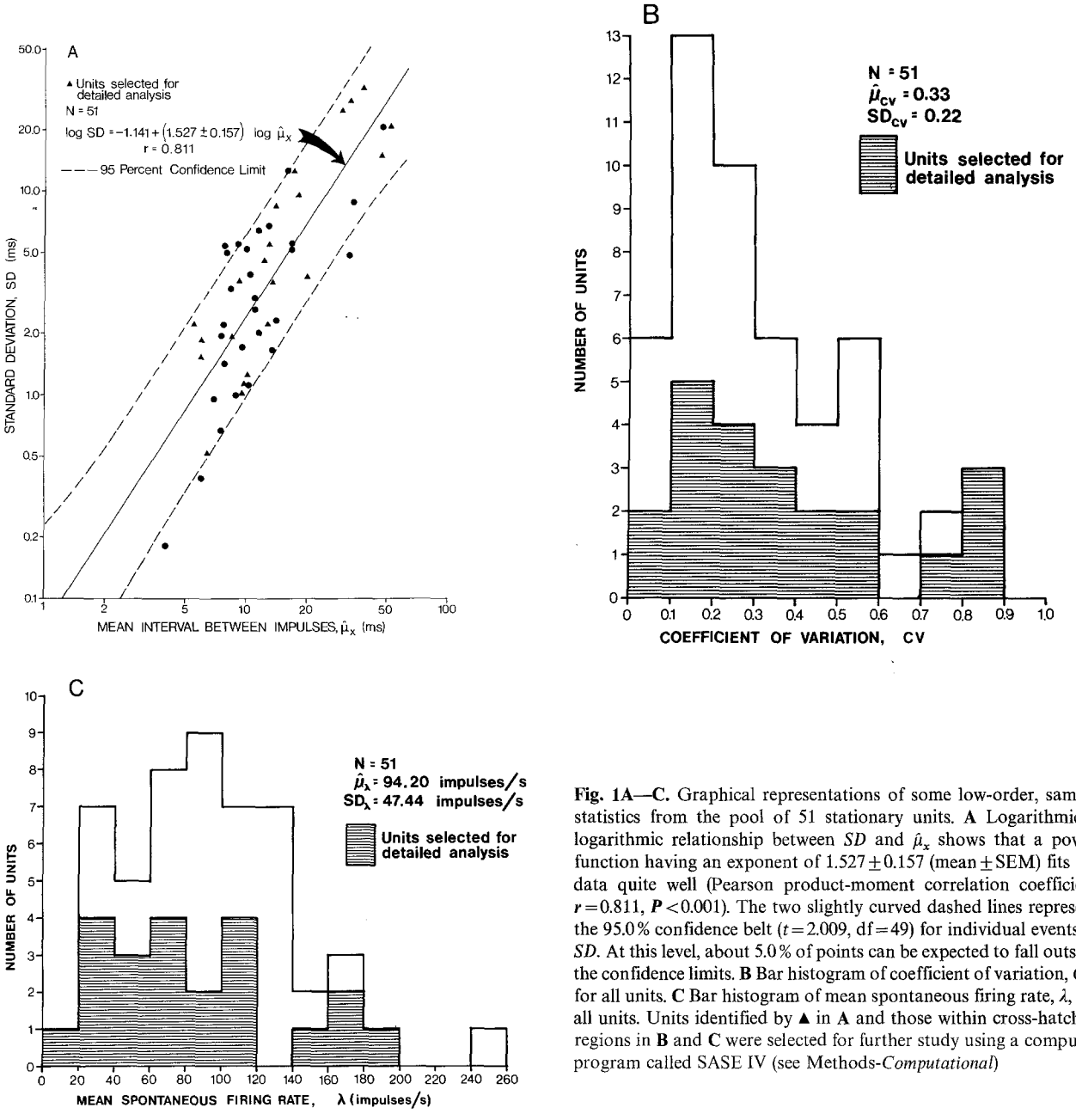

Fig. 1A—C. Graphical representations of some low-order, sample statistics from the pool of 51 stationary units. **A** Logarithmic—logarithmic relationship between *SD* and $\hat{\mu}_x$ shows that a power function having an exponent of 1.527 ± 0.157 (mean $\pm$ SEM) fits the data quite well (Pearson product-moment correlation coefficient $r = 0.811$, $P < 0.001$). The two slightly curved dashed lines represent the 95.0% confidence belt ($t = 2.009$, df = 49) for individual events in *SD*. At this level, about 5.0% of points can be expected to fall outside the confidence limits. **B** Bar histogram of coefficient of variation, *CV*, for all units. **C** Bar histogram of mean spontaneous firing rate, λ, for all units. Units identified by ▲ in **A** and those within cross-hatched regions in **B** and **C** were selected for further study using a computer program called SASE IV (see Methods-*Computational*)

distribution function $(nD_n)^{1/2}$ and it specifies that a rejection of distributional equality is false. The Williams and Kloot test (Himmelblau, 1970) was employed to provide a *t*-test and determine statistically significant differences between best-fitting models.

Results

Spike Train Stationarity

The Wald-Wolfowitz runs test evaluates conditions of weak stationarity. When this test was applied to our sample of 120 neural units, the presence of a trend (Z, $P < 0.01$) was noted in 69 units (57.5%), while no trend was indicated in the remaining 51 units (42.5%). When the spike train sample was sectioned into "quarters" (see exact record length in Methods-*Computational*), we found that, for all but two units, stationarity was maintained in each quarter as well as for the total record length in the case of the 51 stationary units. In contrast, of the 69 units showing a non-stationarity in their overall neural firing patterns, a total of 40 units (58.0%) gave indication of a trend in one or more of their quarter data segments. (This figure is increased to 76.8% for a level of significance $P < 0.05$.) These results indicate that short-term trends appear to carry over

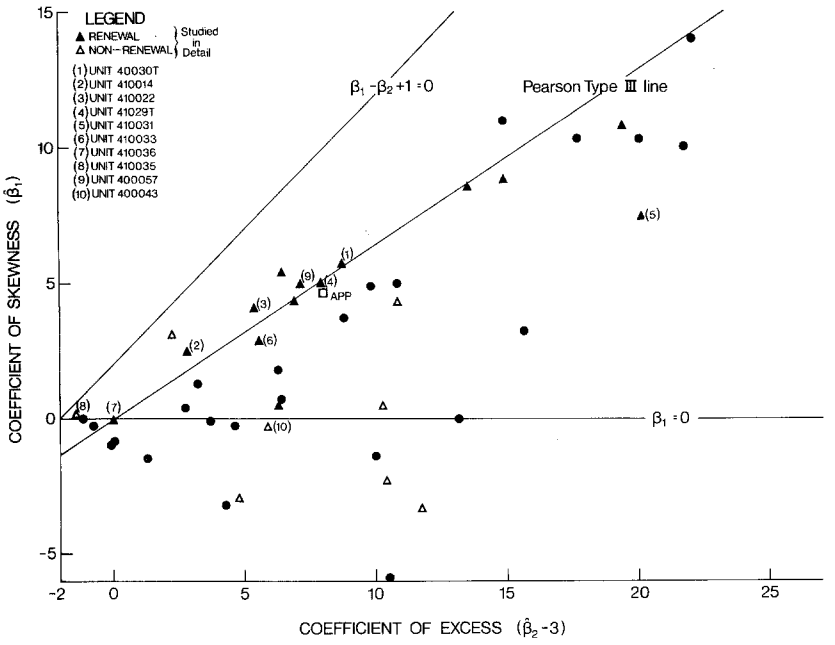

Fig. 2. Plot of coefficient of skewness ($\hat{\beta}_1$) versus coefficient of excess ($\hat{\beta}_2 - 3$) ($\hat{\beta}_2 \equiv$ coefficient of kurtosis) for 46 stationary units and the APP. The line $\beta_1 - \beta_2 + 1 = 0$ represents the theoretical upper boundary for units characterized by the Pearson system of frequency curves (Pearson and Hartley, 1970)

into long-term trends in the majority of the non-stationary units that we analyzed. In contrast, the stationary units tend to be trend-free throughout regardless of their sample length sizes.

First-Order Statistics

For the 51 stationary units, $\hat{\mu}_x$ varied from 4.00 ms to 51.22 ms, with an average of 15.06 ms and a standard deviation of 11.38 ms. The SD's of these units range between 0.18 ms (for a very regularly firing unit) and 32.07 ms (in a unit displaying considerable spread about its $\hat{\mu}_x$). The relationship between SD and $\hat{\mu}_x$ for these units is shown in Figure 1A and can be expressed in the form

$$SD = 0.0722\,\hat{\mu}_x^{(1.527 \pm 0.157)}. \tag{17}$$

Histograms of the number of units versus their CV and λ are shown in Figures 1B and C, respectively. All units had a $CV < 1.0$ (range -0.05—0.88). Values of $\hat{\beta}_1$ versus $(\hat{\beta}_2 - 3)$ are shown in Figure 2 for 46 of the stationary units. The majority of the neural units fall into two distinct groups, one about the Pearson Type III line (Pearson and Hartley, 1970) (irregular units) and the other about the line of negligible skewness, $\beta_1 = 0$ (regular units). It is important, however, to note that there are some units which lie outside these two extremes and cannot be clearly classified as having either regular or irregular spontaneous activity. Units at the intersection of the Pearson Type III line and the line, $\beta_1 = 0$, have intervals which can be described by a normal (Gaussian) distribution. Units directly on the Pearson Type III line *theoretically* should display ISIs characteristic of the gamma distribution (*vide infra*).

The 22 stationary, spontaneously-active units, which were analyzed using SASE IV, were selected on the basis of their positions on the chart of β_1 versus $(\beta_2 - 3)$ (denoted by △ and ▲ in Fig. 2), and were chosen because they seemed to represent a range of distribution patterns. We have also indicated the position of these units on the plot of SD vs $\hat{\mu}_x$ (Fig. 1A) and have shown their relevant λ's (Fig. 1C) and CV's (Fig. 1B). From these figures, it appears that the sample chosen is a representative one.

Tests for Poisson Process

The V-statistic is an optimum test of the alternative hypothesis of a Poisson process having a time-varying parameter, $\lambda(x)$, of the form indicated in (5). For all 22 units and the APP, the hypothesis of a time-dependent process of this form was rejected ($\boldsymbol{P} > 0.05$). The V-statistic detects only a linear form of time-dependency with the assumption that the intervals x_i are independent and exponentially distributed. The Wald-Wolfowitz runs test, however, is not sensitive to the form of $\lambda(x)$ nor the distributional properties of the intervals; and, therefore, is more appropriate as an overall test for vaguely specified non-stationary alternatives.

The results of the Kolmogorov-Smirnov and Anderson-Darling tests to the quantities derived from (6) and (7) are presented in Table 1. The most striking observations are that, when the Y_i-quantities are evaluated by the one-sided Kolmogorov-Smirnov ($\boldsymbol{YKS}^-$

Table 1. Results of statistical tests for Poisson and renewal processes

Unit	Ser. corr. coef.			Exponential scores			Tests for Poisson process				Tests for renewal process		
	$\hat{\varrho}_1(n-1)^{1/2}$	$\hat{\varrho}_2(n-2)^{1/2}$	$\hat{\varrho}_3(n-3)^{1/2}$	$\hat{R}_1$	$\hat{R}_2$	$\hat{R}_3$	YKS^-	YAD	WKS^-	WAD	CKS^-	CAD	M
40230T	2.51	1.65	1.70	1084.1	1093.5	1075.1	0.113	0.130	23.493*	1313.586*	1.608*	4.930*	0.035
41029T	0.68	0.70	0.08	1046.3	1053.2	1034.8	0.335	2.161	14.656*	295.807*	0.791	1.127	0.274
40030T	1.30	0.79	2.78*	1064.7	1046.3	1102.4	0.724	0.913	5.450*	53.173*	1.292	2.067	0.612
410157	3.56*	−1.38	−0.31	1048.9	987.9	1057.4	0.042	0.057	27.107*	—	1.835*	7.255*	0.022
400160	4.13*	−0.64	0.39	1067.9	1003.8	1039.1	0.144	0.020	27.459*	—	2.287*	10.098*	0.017
410036	−0.92	−0.15	0.06	976.9	1021.6	1024.5	0.090	0.019	26.334*	1851.990*	0.449	0.867	0.014
400051	4.54*	1.45	1.89	1137.2*	1125.4*	1094.5	0.086	0.351	23.348*	1367.948*	2.140*	11.653*	0.0001
400043	8.20*	0.29	0.82	1197.8*	1072.8	1106.7*	0.037	0.235	24.210*	1331.375*	3.840*	36.725*	0.0002
410042	0.99	0.30	0.41	1074.2	1060.6	1025.8	0.102	0.423	23.429*	930.638*	0.833	0.868	0.101
410076	0.20	0.10	−2.45	1028.8	1028.4	948.8	0.387	0.241	20.129*	—	0.650	0.672	0.156
410035	0.28	4.67*	4.02*	1035.3	1116.3*	1086.9	0.178	0.478	29.731*	—	1.856*	6.002*	0.008
400003	3.79*	1.89	0.52	1138.9*	1094.3	1036.0	0.804	0.752	10.629*	130.525*	2.233*	7.585*	0.549
410005	1.38	2.88*	0.67	1063.0	1093.2	1044.9	0.232	0.136	22.014*	779.750*	1.282	2.827	0.146
410022	−1.35	−1.42	−0.07	978.2	976.8	1005.2	0.111	0.106	21.661*	672.339*	0.302	1.563	0.114
400024	−0.30	2.19	−0.64	1005.9	1055.1	1039.0	0.106	0.046	25.565*	1437.316*	0.796	1.683	0.049
410014	1.34	−1.42	−0.46	978.2	976.8	1005.2	0.637	0.446	5.245*	56.967*	0.260	1.557	0.608
400072	0.45	0.20	−0.16	1045.3	1041.3	1044.8	0.204	0.836	18.378*	425.343*	0.647	0.498	0.215
400061	−0.54	−0.03	−1.79	930.0	1023.8	968.4	0.295	0.141	24.337*	1447.201*	0.389	0.553	0.027
400060	5.13*	0.01	−0.92	1089.5	1053.2	1001.6	0.198	0.040	25.934*	1754.387*	2.745*	13.559*	0.100
410033	0.02	0.64	2.25	1011.1	1056.6	1102.7	0.508	0.303	18.277*	707.878*	0.879	1.187	0.097
400057	0.96	0.60	−0.37	1052.3	1041.5	1006.8	0.396	0.351	7.782*	70.859*	0.762	0.815	0.568
410031	0.08	0.09	0.26	1005.3	1043.9	1030.8	0.239	0.273	16.282*	540.846*	0.478	0.328	0.165
APP	1.35	−0.47	0.45	1067.5	1007.6	1033.1	0.474	0.280	0.525	0.567	0.923	1.525	1.099

Score statistics of 1105.7, 1104.3, and 1103.9 for R_1, R_2, R_3, respectively, at $P=0.01$ level of significance have been linearly interpolated from values given by Lewis and Goodman (1968). The 1% asymptotic significance point for the Kolmogorov-Smirnov (KS^-) statistic is 1.518, for the Anderson-Darling (AD) statistic it is 3.857 (Cox and Lewis, 1966), and for the Moran statistic (M) it is 1.105. All *-entries are significant ($P<0.01$)

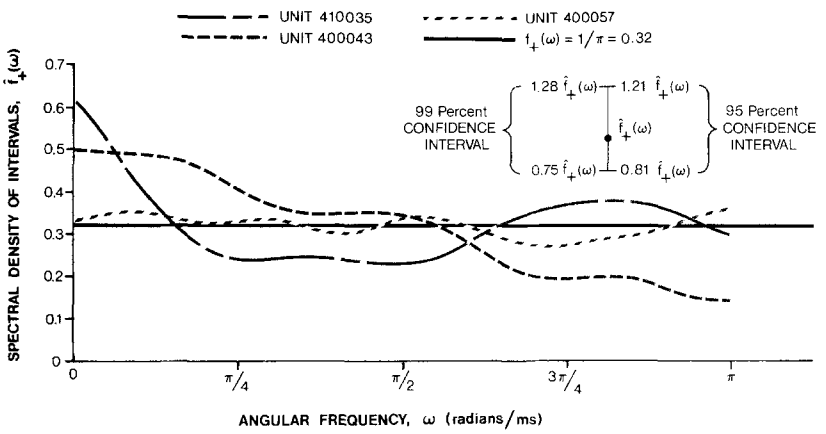

Fig. 3. Estimated spectral density of intervals for three units. Estimates are based on the first $m = 20$ serial correlation coefficients in each instance. Higher values of m do not show distinguishable features other than those apparent at this level. The approximate coefficient of variation of individual estimates of $\hat{f}_+(\omega)$ is $(m/2n)^{1/2} = 0.10$. Jenkins and Watts (1968) show that $v\hat{f}_+(\omega)$ is distributed according to a χ^2_v-distribution, where $\mathrm{df} \equiv v = 3.71\ n/m$ for a Parzen lag window. This feature may be used to derive confidence limits for $\hat{f}_+(\omega) = 1/\pi$. The 95.0 and 99.0% confidence intervals for this $\hat{f}_+(\omega)$ are shown for $v = 190$ df and are frequency dependent. Consequently, it is necessary to multiply the upper (1.21 or 1.28), and lower (0.81 or 0.75) limits by the appropriate values of $\hat{f}_+(\omega)$ in order to obtain the exact limits for each curve at a particular ω

in Table 1) and the Anderson-Darling (***YAD*** in Table 1) tests, the Poisson hypothesis was accepted in all instances. However, when the W_i-quantities were used there was a strong rejection of the Poisson hypothesis in all 22 cases, to both the Kolmogorov-Smirnov (***WKS***$^-$ in Table 1) and Anderson-Darling (***WAD*** in Table 1) goodness-of-fit tests. Although both test statistics cause a strong rejection of the W_i-variates, the ***WAD*** statistics show a much more convincing rejection than do the ***WKS***$^-$ entries (cf. Lewis, 1961). It is conjectured that the Anderson-Darling test is much more affected by deviations in the tails of the distribution functions than is the Kolmogorov-Smirnov test (Cox and Lewis, 1966). In practice, there is usually a paucity of empirical data points in the tails of the distributions; and, consequently, the stronger rejection of the Poisson hypothesis by the Anderson-Darling test is not unexpected. Note also that, as expected, the APP does not give any strong indication of a departure from the Poisson hypothesis with both test statistics.

Although the W_i-quantities cannot be expected to increase the power for rejection of a false null hypothesis with all alternatives, it is conjectured that there is an increase in power against most alternatives. A specific case where this advantage over the unmodified variates is apparent is as a *test for the Poisson hypothesis in trend-free data* (Lewis, 1965). As has already been shown, the 22 units were found to be stationary (trend-free) when tested by both the Wald-Wolfowitz runs test and the V-statistic. Thus, the absence of a trend in our spike train data must be considered a major factor in causing the striking disparity between the results of the two variates. Because of this, we feel that the W_i-quantities (which, when tested, indicate rejection of the Poisson hypothesis) are more appropriate quantities to test our data.

Tests for Renewal Process

Central to any test for a renewal process is the problem of the independence of the intervals. It is difficult to establish a renewal process's authenticity, primarily because the alternative hypotheses are hard to specify. For this reason, it is advisable to use a number of tests in order to increase the likelihood of finding a correct interpretation of the results. Both the statistics, $\hat{\varrho}_j(n-j)^{1/2}$ and $\hat{R}_h$, are useful in this regard and are based on the properties of the joint distribution of intervals. By making the assumption that these statistics can be approximated by a normal distribution, we found that only 6 of the 22 units (Table 1) had their standardized normal variate, $\hat{\varrho}_1(n-1)^{1/2}$, significantly different from zero ($\boldsymbol{P} < 0.01$). In all, only 9 units gave an indication of a dependency between intervals in one or more of the first three serial correlation coefficients. There is less evidence of a serial dependency between intervals from the results of the $\hat{R}_h$'s. However, it is noteworthy that the 4 units having at least one of their three $\hat{R}_h$'s significantly different from zero ($\boldsymbol{P} < 0.01$—see Table 1) also demonstrated this feature with the $\hat{\varrho}_j(n-j)^{1/2}$'s. As expected, values for the APP were well within the 1% significance levels for both statistics; therefore, interval dependency was rejected.

A major disadvantage in using $\hat{\varrho}_j(n-j)^{1/2}$ is that measurement errors (Shiavi and Negin, 1973) or local or global trends (Perkel et al., 1967) may introduce signi-

Table 2. Best-fit statistics to probability density functions of selected units having properties of a renewal process

Unit	RMSE(%)				P_{KS}		Williams and Kloot[a]
	WL fpt	Gamma	Exponential	Exponential -with-delay	WL fpt	Gamma	
40030 *T*	0.21	0.26	0.43	0.43	0.711	0.000	6.83 (251)[c]
410014	0.25	0.26	0.47	0.46	0.034	0.024	0.61 (149)
410022	2.52	2.81	9.69	9.53	0.000	0.000	3.97 (17)[c]
41029 *T*	0.96	1.08	6.34	6.29	0.000	0.000	7.49 (84)[c]
410031	0.18	0.20	0.65	0.65	0.017	0.000	4.69 (253)[c]
410033	0.25	0.27	0.99	0.97	0.226	0.011	3.81 (155)[c]
410036	0.94	[b]	14.51	[b]	0.567	[b]	107.60 (11)[c]
Average RMSE $\pm$ SEM (%)	0.76 ± 0.32	0.81 ± 0.42	4.73 ± 2.13	3.06 ± 1.59			

[a] Comparison is between LSEs (to 6 decimal places) of WL fpt pdf and gamma pdf. Entries are *t*-values and df (in parentheses), respectively
[b] Unable to fit pdf in 500 computer iterations
[c] WL fpt pdf is a significantly better fit ($P \leqq 0.05$ with 2-sided *t*-test) than is the gamma pdf

ficant serial dependency between the ISIs and therefore mask the state of the true conditions. Tests based on the spectrum of intervals, i.e., the C_j-quantities [see (8)], appear to be insensitive to some of the effects described above (Perkel et al., 1967). Both the one-sided Kolmogorov-Smirnov (***CKS***$^-$ in Table 1) and Anderson-Darling (***CAD*** in Table 1) tests give strong evidence that the criterion of independence of intervals is not significantly different from that expected for a renewal process ($P < 0.01$) in 63.6% of units investigated. Moreover, the results show that there does not appear to be a preference in choosing one statistic over the other. Interestingly, of those units demonstrating an interval-dependency with this test, 87.5% had previously shown a significant serial correlation and 50.0% a significant exponential score (cf. entries in Table 1). As expected, there was no rejection of the hypothesis of a renewal process in the case of the APP.

Plots of $\hat{f}_+(\omega)$ give a qualitative picture of the periodicity in a process and, *ipso facto*, the degree of departure from a renewal process. For example, Unit 400057 shows very small deviations from the value for a renewal process, $\hat{f}_+(\omega) = 1/\pi$ [requires that $\hat{\varrho}_j = 0$ in (2)], throughout its entire spectrum and is well within the 95.0% confidence limits (Fig. 3). The smoothed spectra for Units 410035 and 400043 in Figure 3, however, show considerable departures from the line, $1/\pi$, with both 95.0 and 99.0% confidence intervals over much of the length of the curves. The large values at low ω's are the result of many positive $\hat{\varrho}_j$'s to large lags in the case of Unit 410035. The magnitude of $\hat{\varrho}_1$ (cf. Table 1) for Unit 400043 is so much more significant than that of its neighbors (which tend to cancel when summed) that its contribution to $\hat{f}_+(\omega)$ is considerable at two distinct points on the spectrum, one at $\omega = 0$ and the other at $\omega = \pi$. Plots of $\hat{f}_+(\omega)$ for other units further substantiate the conclusions we have drawn from the statistical tests in Table 1.

Using the tests described herein, there appears to be a high correspondence between a unit's location on the coordinate plot of $\hat{\beta}_1$ vs $(\hat{\beta}_2 - 3)$ (Fig. 2) and its likelihood of having the properties of a renewal process. More specifically, 7 out of 8 units (87.5%) which appear to be representative of a renewal process are found to be clustered in a region which originates at the point (0, 0) in the plot, and through which the Pearson Type III line passes. [Of the remainder, only 1 of 7 units (14.3%) is representative of a renewal process.] This suggests the need for a test for the Poisson process against a renewal alternative in which the ISIs are independent and distributed according to a gamma pdf. The asymptotically most powerful test against this renewal alternative is the Moran statistic, ***M***, values of which are shown in Table 1 for each of the 22 units and the APP. In all instances, the Poisson hypothesis was accepted as against the renewal alternative ($P > 0.01$). Thus, it appears unlikely that the underlying distributions are independent and gamma-distributed. Confirmation of this fact is provided in Table 2, where the gamma, exponential, and exponential-with-delay pdfs were fitted to ISI histograms of the seven units discussed above and found to be "bad" fits when compared to the fit of the more general WL process [see (15)]. Fits of these pdfs to Unit 40030T are shown in Figure 4 as an example.

The Second-Order Properties of the Counting Process

Second-order properties indicate interesting information regarding the nature and origin of regular and irregular vestibular discharge patterns. In Figures 5 and 6, we compare the results of $\hat{g}(k\gamma + \gamma/2)$, $\hat{Var}[t]$, and $I(\ell')$

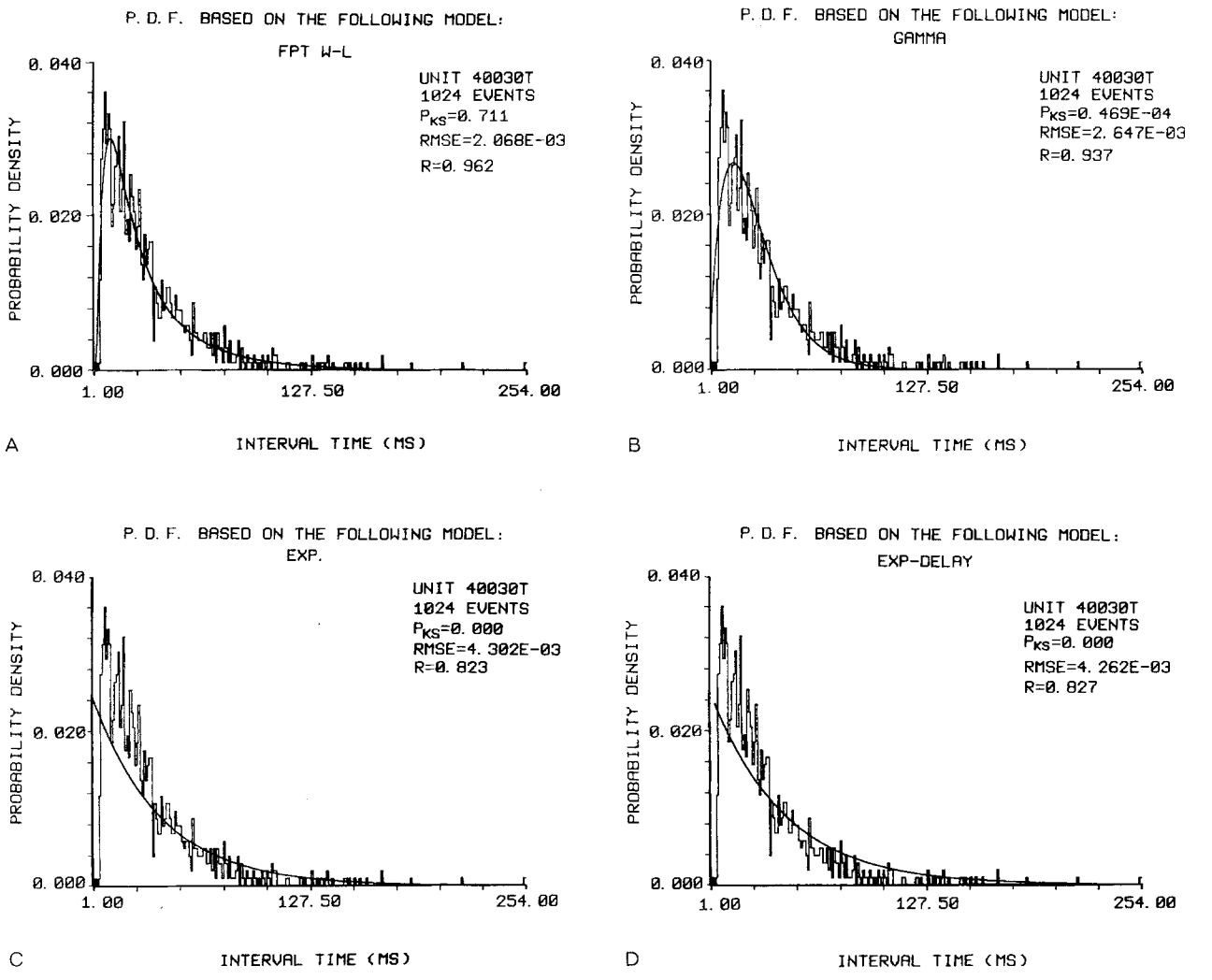

Fig. 4A—D. Best-fitting pdfs to ISI histogram of Unit 40030T. **A** Fit of WL fpt pdf ($P_{KS}=0.711$, RMSE = 0.21%, $R=0.962$). **B** Fit of gamma pdf ($P_{KS}=0.000$, RMSE = 0.26%, $R=0.937$). **C** Fit of exponential pdf ($P_{KS}=0.000$, RMSE = 0.43%, $R=0.823$). **D** Fit of exponential-with-delay pdf ($P_{KS}=0.000$, RMSE = 0.43%, $R=0.827$). The coefficient of determination, R, relates the variance produced by lack of fit of pdf (MSE) to the variance of the ISIs ($V_{\hat{p}}$) about their mean and can be expressed as $R=\pm(1-\mathrm{MSE}/V_{\hat{p}})^{1/2}$

for Units 40030T (an irregular unit) and 410035 (a regular unit). It is quite obvious, from the empirical expectation density in Figure 5A, that the Poisson prediction breaks down at the shorter time intervals for Unit 40030T. This behaviour, however, is quite consistent with that expected for certain other forms of the renewal process. For instance, the expectation density for the WL process with absorbing barrier for this unit (and whose pdf is shown in Fig. 4A) deviates from the Poisson prediction in a manner similar to that obtained empirically at the shorter time intervals.

While the expectation density provides its main information at the shorter time intervals, the variance-time curve is interesting because of its form for large times. Consequently, we considered the asymptotic form of $Var[t]$ for the renewal process; i.e., we used the form $Var[t] \simeq \{(CV)^2 nt/s_n\} + K$ [where K is an appropriate constant, which involves the higher-order moments of the process—see p. 81 in Cox and Lewis (1966)]. When the appropriate parameters are used for the WL process in this equation, the asymptotic form of $Var[t]$ is seen to fit the data quite well (Fig. 5B). This particular unit happens to have a large $CV(=0.87)$; a value not unlike that obtained from the experimental data of a Poisson process. Thus, it is not surprising that both experimental curves—$Var[t]$ for a Poisson process in which the mean interval of the data was used; and the asymptotic form of $Var[t]$ for a renewal process in which the parameters of the best-fitting WL fpt pdf were used—fall within the confidence limits of the Poisson process prediction. This is most fortunate because we can now predict with the same confidence

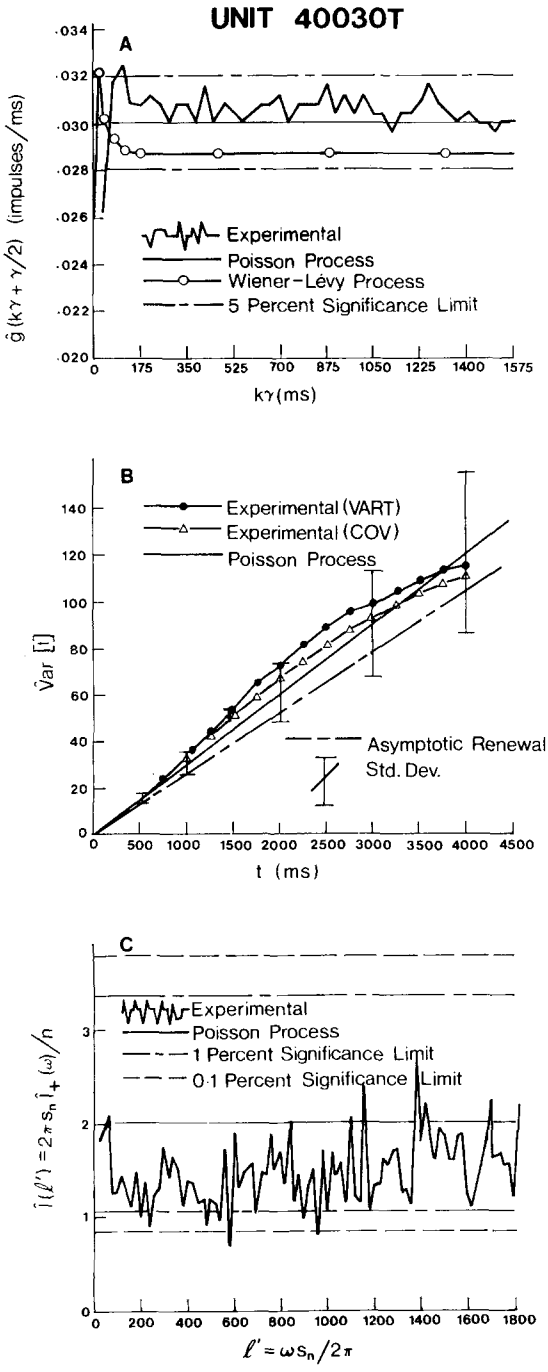

Fig. 5. A Empirical expectation density, smoothed over an interval 2γ, where $\gamma = 35$ ms. Although the significance limits actually diverge with increasing $k\gamma$, the number of estimates shown are too few to demonstrate this unequivocally. There are significant initial departures in $\hat{g}(k\gamma + \gamma/2)$ from the constant value $n/s_n = 0.030$ impulses/ms for a Poisson process; a result consistent with that expected from the expectation density of a WL process fitted to the data. The curve for the WL process has been determined according to $g(x) = 2.49x^{-3/2}e^{-0.016} \sum_{\ell=1}^{85} \exp\ell\left[\frac{-19.47\ell}{x} + 1.12\right]$, using the appropriate parameters. Deviations between theoretical and experimental curves are due to sampling errors in the estimation of the parameters of the WL fpt pdf and to a less than optimum choice of γ in $\hat{g}(k\gamma + \gamma/2)$. For $k\gamma > 100$ ms, both experimental and theoretical curves are confined within the significance limits for a Poisson process. **B** Experimental data for variance-time curves have been determined in two different ways, both of which are shown. Standard deviations for a Poisson process are based on (14) with $\Delta = 25$ ms. In general, the experimental points fall within limits of ± 1 standard deviation of $Var[t] = nt/s_n = 0.030t$ for a Poisson process. This is not surprising given the fact that $CV = 0.87$. Using the fitted parameters to the fpt pdf of a WL process, the asymptotic renewal form, $Var[t] \simeq 0.026t$ (K is negligible). This is comparable to the results derived from the data, i.e., $Var[t] \simeq 0.023t$ (not shown above). **C** Estimates of $I(\ell')$ have been obtained by a 20-point uniform weighting scheme. A significant number of the estimates are less than the value 2.0 for a Poisson process with a 1.0% significance limit

that the WL process with an absorbing barrier is a good model to this data.

Very little can be said about the spectral density of the counting process for Unit 40030T, other than that a large number of its values exceed the lower 1.0% significance limit for a Poisson process for which the expected value $\hat{I}(\ell') = 2.0$ (see Fig. 5C). However, the form of $\hat{I}(\ell')$ for Unit 40030T is interesting because it differs so strikingly from the form expected from units having non-renewal properties and located on the line, $\beta_1 = 0$, in the Pearson system of frequency curves. For example, $\hat{I}(\ell')$ for Unit 410035, which is typical of this latter type of unit (see Fig. 2), has as its main characteristic a series of sharp peaks; the first of which corresponds to the mean frequency of impulse firing, λ, for the almost periodic spike train, and the remaining ones which are multiples of that λ. As indicated in Figure 6A, the 1.0% significance limits for a Poisson process are quite meaningless for such a unit.

The results of $Var[t]$ for Unit 410035 (see Fig. 6B) are also quite interesting because the curve increases steadily at first and then flattens out to a constant value, $D = 4.758$, at $t \simeq 1100$ ms. Furthermore, the theoretical curves of $Var[t]$ in Figure 6B demonstrate, quite clearly, that the Poisson and renewal processes appear to be inappropriate models to describe the impulse-generating mechanism in those neural units typified by Unit 410035 (regular unit).

Discussion

Pertinent Neuromorphological and Electrophysiological Observations

Information from electron photomicrographs has provided a reasonably complete picture of the types of synaptic contact that occur in the mammalian vestibular neuroepithelium (Engström et al., 1972; Iurato and Taidelli, 1964; Smith and Rasmussen, 1968). The primary afferent innervation of the Type I hair cell is by means of a nerve calyx which forms a shell around a single cell. One or more bouton-type endings (pre-

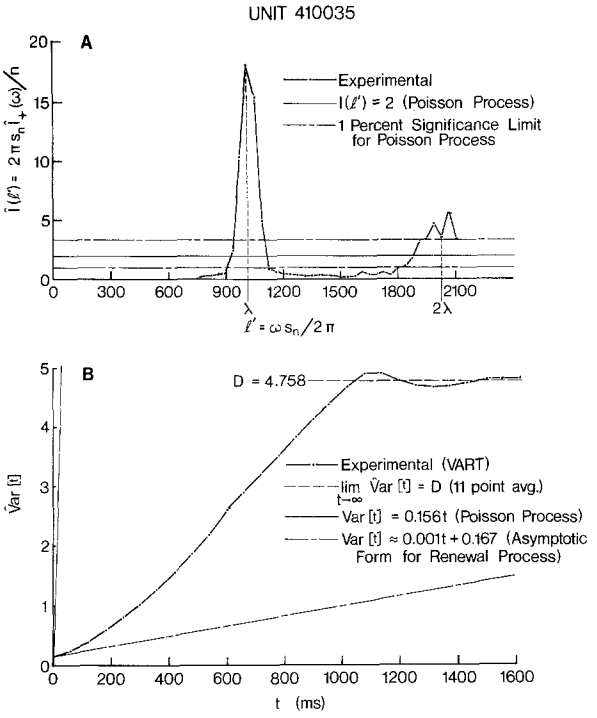

Fig. 6. A Normalized spectral density of the counts (action potentials). Very little of the spectrum falls within the 1.0% significance band for a Poisson process. The first peak in $I(\ell')$ occurs at a frequency, $\lambda = 1013/6.546 = 154.75$ impulses/s, a value comparable to the mean frequency of impulse firing ($= 156.49$ impulses/s) from the raw data. Other peaks occur at 2λ (shown in figure), 3λ, etc. **B** The estimate, $\hat{V}ar[t]$, indicates that the experimental data are more ordered than is expected for a Poisson process. (For this unit, we have not plotted the standard deviation of $\hat{V}ar[t]$ for a Poisson process since its inappropriateness as a model is self-evident.) The plot also shows that the asymptotic form for a renewal process does not fit the data except for very small t. For large t, $\hat{V}ar[t] = D = 4.758$, i.e., it approaches a constant value. (D was calculated by averaging the final 11 values of $\hat{V}ar[t]$, all of which appear to define a trend towards a constant value in the experimental variance-time curve)

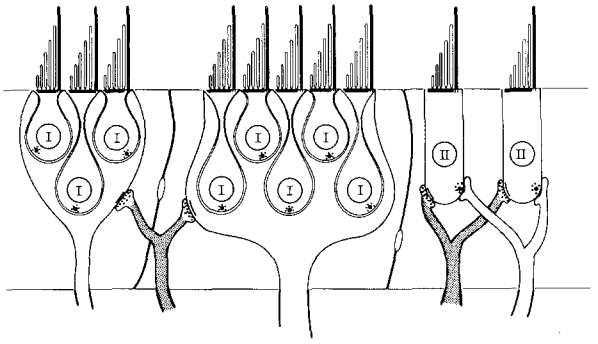

Fig. 7. An illustration of the most common forms of the Types I and II hair cells, and their efferent (shaded) and afferent innervation in the bird. Several Type I hair cells may be enclosed within a single nerve chalice. Densely vesiculated (dots within nerve terminals), synaptic boutons from efferent fibers form connections with the somas of the Type II hair cells and the nerve chalices (calyces) of the Type I hair cells. The nerve chalice, which completely encloses the basal portion of several Type I hair cells and makes synaptic contact with them, represents the most distal part of the afferent fiber system. The afferent connections to each Type II hair cell consist of one or more bouton endings, each of which may result from a single or a branching nerve fiber. Structures which are associated with neurochemically-transmitting synapses are indicated within the hair cells and chalices. The horizontal line at the bottom of the figure, through which the nerve fibers penetrate, portrays the basement membrane—the region at which each nerve fiber loses its myelin sheath (thickened portion) before entering the neuroepithelium. It is believed that the initial myelinated segment of the afferent nerve fiber is the area in which the action potential originates, i.e., it is the spike-initiating locus (SIL). All of the hair cells shown have at their apical ends small tufts which are comprised of a single kinocilium (dark vertical bar) and many stereocilia; the latter of which increase in height in the fashion of a pipe organ in the direction of the kinocilium. It is believed that these cilia sense and transfer mechanical energy resulting from head motion to the hair cell where the neural transduction process occurs (modified from Jørgensen and Andersen, 1973)

sumably from small efferent fibers) always synapse on or near the nerve calyx. In the otolithic maculae and sensura neglecta of Aves, it is more common to find several cells enclosed within a single calyx (Fig. 7). In fact, up to 12 Type I hair cells may be enclosed within the same nerve chalice (Jørgenson and Andersen, 1973). On the basis of their studies on the isolated fowl embryo otocyst, Friedmann and Bird (1967) suggest that each individual calyx in the cristae *should* contain more than one hair cell. Using light and transmission electron microscopy, we have demonstrated that many calyces in the bird's cristae do contain multiple Type I hair cells (unpublished observations). For the Type II hair cells, the most common pattern of innervation is substantially different from the classical pattern that has been described for Type I cells. As shown in Figure 7, one or more afferent and efferent fibers make synaptic contact by means of bouton-endings with a typical Type II hair cell. Furthermore, it appears that several Type II hair cells may be innervated by the same efferent fiber (Wersäll, 1956; Iurato and Taidelli, 1964; Smith and Rasmussen, 1968) by means of boutons *en passant*. Thus, it seems likely that some of the unit activity recorded from Scarpa's ganglion in this study is the result of contributions from several of these source generators. It must be emphasized that this complex branching only occurs in the *unmyelinated* portions of the neuroepithelium. It has been suggested (Flock, 1971) that, for the neuroepithelia of the vestibular and auditory systems, action potentials originate at the point at which the primary afferent fibers become myelinated, i.e., in the area where they leave the basement membrane. Thus, it seems reasonable that there should be considerable spatiotemporal summation of synaptic potentials at the spike-initiating locus (SIL) of the afferent fiber.

Morphological similarities exist between the hair cells and their synaptic organization in the auditory,

vestibular, and lateral-line organs of most vertebrates. Furthermore, these hair cells are homologous from an evolutionary point of view (Flock, 1971). This is fortunate, because information about the diverse properties of the hair cell-nerve junction complex is often more readily obtainable from the more easily accessible lateral-line organs than it is from the vestibulo-cochlear apparatus in higher-order vertebrates. Recently, potentials have been recorded from the base of the hair cells in the lateral-line organs of the salamander, *Necturus maculosis* (mudpuppy) and the fresh-water cod, *Lota lota* (burbot), and the macula sacculi of the goldfish, *Carassius auratus* (Furukawa and Ishii, 1967; Ishii et al., 1971; Furukawa et al., 1972; Flock, 1971; Flock and Russell, 1973a,b, 1976) which have been identified as postsynaptic potentials (PSPs).

Spontaneous miniature potentials having a 0.32 ($\pm$0.16) mV mean ($\pm$ standard deviation) amplitude and an approximate, half-width duration of 0.5 ms were identified by Furukawa et al. (1972) as excitatory postsynaptic potentials (EPSPs). These EPSPs could be augmented in both magnitude and duration (leading to a summation of the EPSPs) with a hyperpolarizing current and they diminished in size with a depolarizing current. Ishii et al. (1971) considered these EPSPs to result from the quantal secretion of a neurochemical transmitter substance across a synapse and into the afferent bouton where the potentials were produced.

Flock and Russell (1973b) discovered that, *during* efferent nerve fiber stimulation, large hyperpolarizing potentials could be recorded which they identified as inhibitory postsynaptic potentials (IPSPs). Concomitant with these recordings was an increased conductance of the postsynaptic membrane of the hair cell, which they felt indicated the release of an inhibitory neurotransmitter substance. EPSPs recorded from the afferent ternimals were substantially reduced during efferent nerve stimulation. They suggest that the effect of the IPSPs is to decrease the amount of excitatory neurotransmitter at the afferent synapse, presumably because of a shunting of excitatory current through the efferent postsynaptic membrane. As in inhibitory synapses in other neural structures, the IPSPs tend to drive the membrane potential toward the resting potential of the hair cell which results in a decrease in activity in the afferent fibers (Flock and Russell, 1976).

Relevance of Candidate pdfs *to Spike Initiation*

In a neurophysiological context, the gamma pdf can be considered a pure threshold model with the property that discrete excitatory potentials (pulses) impinge on the SIL of the hair cell and sum temporally (without decay) up to a constant threshold level at which point an action potential is generated. The membrane potential of the neuron is then reset instantaneously to its unenergized condition and the process starts over again as soon as the next excitatory pulse arrives. The excitatory stimuli appear in a random manner (Poisson process) with a mean frequency, λ, and the neuron discharges whenever δ pulses occur. Thus, the so-called waiting times to impulse generation are represented by a gamma pdf [see (10)]. If the excitatory pulses arrive at the SIL in a Poissonian manner, and each individual pulse is capable of causing the membrane potential to reach threshold and fire the neuron, then the output spike train is also a Poisson process with waiting times expressed by an exponential pdf [$\delta = 1$ in (10)]. Poisson processes are memoryless, i.e., the appearance of each event is completely independent of the appearance of any other event. In a neurophysiological context, this property is not necessarily evident. In particular, the inherent absolute refractory time that is associated with the generation of an action potential and which produces a "dead" time necessitates a modification to the exponential pdf. The resulting form, the exponential-with-delay pdf, has been shown to provide a good fit to the ISIs from the spontaneous activity in peripheral cochlear units (Kiang et al., 1965; Walsh et al., 1972). In contrast, we have shown that neither the Poisson process (see Table 1) with its realization, the exponential pdf, and the exponential-with-delay pdf or the gamma pdf (cf. Table 2) appear to be appropriate models for the vestibular apparatus.

A process more appropriate to the vestibular apparatus might be the WL process which can be considered analogous to a drifting membrane potential at the SIL which moves, without decay, toward a threshold level (absorbing barrier), at which point an action potential is produced, with the subsequent return of the membrane potential to its resting level from which the process starts over again. The ISI distribution obtained from the resulting spike train is associated with the times taken for the membrane potential to change from resting to threshold voltage; i.e., it represents the distribution of the fpts of the process. The instantaneous membrane voltage of the SIL is determined by the interaction of two types of input effects—one contributing EPSPs, which move the membrane potential toward threshold, and the other IPSPs, which move it toward the resting level. A strict application of this process requires that the EPSPs and IPSPs are small relative to the threshold level; that they occur at a high frequency compared to the mean spontaneous firing rate; and that they occur with almost equal probability.

In a variety of neurons in which it would appear that the WL process can be strictly applied, the threshold level ranges from 10 to 40 mV above the resting level,

while the corresponding PSPs have values from 0.5 to 1 mV (Fienberg, 1974). In hair cells, estimates from the data of Furukawa et al. (1972) and Detwiler and Fuortes (1975) place the threshold-to-resting potential difference at 10–20 mV. Spontaneous EPSPs from saccular hair cells in the goldfish appear to have much smaller amplitudes [0.32 mV average—see Furukawa et al. (1972)] than do those in the lateral-line organs of the burbot [0.5–5 mV range—see Flock and Russell (1976)]. Although spontaneous IPSPs for hair cells have not been reported to date, IPSPs down to 2.5 mV amplitude have been recorded when the efferent fibers are stimulated. Moreover, spontaneous action potential activity (presumed to be from the efferent system) with discharge rates of 15–50 impulses/s has been reported (Flock and Russell, 1973a). Thus, it seems reasonable that spontaneous IPSPs should occur in spontaneously active efferent fibers and at rates comparable to those of the spontaneous efferent activity. [Efferent impulses are reduced or completely abolished with anesthetics; their rate increases substantially during or shortly before body movement—see Klinke and Galley (1974).] Estimates from published data indicate that postsynaptic excitatory potentials can occur at rates of 50–250 EPSPs/s in hair cells in fish (Furukawa et al., 1972; Flock and Russell, 1976). Considering that moderate rates up to 25 impulses/s have been reported for the spontaneous afferent action potential activity in fish (Lowenstein, 1956; Hashimoto et al., 1970), one can say, with some confidence, that the EPSPs should occur at a comparatively high frequency compared to the activity in the afferent fibers. Thus, there is evidence that the mechanisms for producing a WL process are present in hair cell receptors. However, it is unlikely that this process occurs in all renewal units in the vestibular neuroepithelium. In fact, the suitability of the WL fpt pdf as a model for the ISI data in our units is demonstrated in only two of the seven select units for which fits were provided ($P_{KS} \geqq 0.5$ in Table 2). It is obvious that, in the absence of IPSPs [since many fibers do not have a spontaneous efferent discharge—see Hashimoto et al. (1970); Klinke and Galley (1974)], the WL process does not hold and a process which relies only on the summation of EPSPs would be more appropriate as a model.

The four candidate pdfs which were used in this study were chosen, in part, for their simplicity and flexibility; and, in part, because they seemingly describe (to a first approximation) the way in which neural activity is generated in the vestibular neuroepithelium. However, these models do not take into account relative refractory effects, variable thresholds, decays in individual PSPs, the hyperpolarized after-potential following an action potential, and the possibility that each spontaneous IPSP completely suppresses the spontaneous afferent activity (e.g., see Fienberg, 1974). The current state of knowledge on spike production in the vestibular neurepithelium is incomplete. Therefore, until there is reliable data to demonstrate the presence of these or other effects, the simple models chosen will have to be sufficient.

Proposed Model of Impulse-Generation in Vestibular Neuroepithelium

From the definition of CV (see p. 200) and (17), it can be shown that, for our units, $CV \propto (\hat{\mu}_x)^{1/2}$ approximately, provided $CV \leqq 1$. Thus, the CV varies as a power function of the mean interval, $\hat{\mu}_x$, of the ISI histograms, i.e., the larger the $\hat{\mu}_x$, the larger will be the corresponding CV. This continuous function suggests that there may be a single basic process at work in the vestibular neuroepithelium; and that, furthermore, this process may be modified according to the location (or required function) of the hair cells. Lifschitz (1973) provides electrophysiological evidence in support of this conjecture. He applied depolarizing and hyperpolarizing direct currents in a stepwise manner (i.e., a staircase-like current waveform) to the membranous ampulla of the lateral semicircular duct in the pigeon, as he simultaneously recorded the extracellular spike activity in the single primary afferent fibers. At each plateau of the applied current, the CV was determined as an indication of the degree of variability of the recorded neural activity. Both the CV and $\hat{\mu}_x$ decreased with increasing amounts of depolarizing currents and, correspondingly increased with increasing hyperpolarizing currents. Similar results were achieved with caloric stimulation. Lifschitz suggested that this similarity exists because caloric stimulation initiates the voltage mechanisms responsible for impulse initiation, whereas the galvanic currents act directly on the afferent terminals in a manner very similar to that of the mechanoelectric transducer process. Extending this argument further, it follows that the probable result of increasing the depolarizing stimulus is the recruitment of an increasing number of hair cells (or synaptic sites). Similarily, the reverse effect would occur with increased hyperpolarization. In the quiescent vestibular neuroepithelium, the range of CV's encountered can only be attributed to the fact that the many individual SILs receive their PSP summation from a differing number of synaptic sites. Since studies show that the afferent fiber diameter can be correlated with the extent to which the terminal ramifications innervate the hair cells (Wersäll, 1956), several investigators have implied that regular discharges (small CV's) occur as a result of multisynaptic bombardments and that irregular discharges (large CV's) result from the involvement of only a few synapses (Goldberg and Fernandez, 1971; Walsh

et al., 1972). This indicates that the range of *CV*'s is possibly dependent on the degree of innervation. Empirical evidence for this argument has been presented by a group of workers (Valli et al., 1973), who showed that, in the frog (which has only Type II hair cells and low levels of spontaneous activity), "spontaneously silent" units in the cristae came from unbranched fibers, whereas those showing spontaneous activity originated from fibers which ramify into several branches within the sensory epithelium. Interestingly, Spoendlin (1972) observed that 95.0% of all afferent fibers to the inner hair cells of the cochlea in cats are unbranched. This is consistent with the hypothesis that an exponential-type distribution of ISIs is produced when one or a few fibers innervate the hair cell (Walsh et al., 1972).

In summary, based on the precision of our measurements and the results of the tests presented herein, we suggest that it is not unreasonable to conclude, that as a first approximation, spike initiation in the vestibular neuroepithelium may be modeled as a renewal process (particularly for irregular discharge patterns). This conclusion allows us to completely describe the process by its first-order properties, i.e., the pdf of a given model. Moreover, we suggest that since a general model such as the WL fpt pdf seemingly provides a good fit to selected ISI histograms, its application to spike initiation in the vestibular neuroepithelium is appropriate; particularly, since there appears to be a neuromorphological and neurophysiological basis for its use in this regard. For these reasons, we conclude that it is possible that the spontaneous discharge patterns which appear in ampullary primary afferents have ISI histograms whose shape is determined by the spatial and/or temporal summation of the EPSPs and/or IPSPs that arise in the neuroepithelium of the crista. Furthermore, the relationship between EPSPs and IPSPs determines the nature of the pdf and, in the absence of the IPSPs (e.g., because of the effects of anesthetics), summation occurs by way of EPSPs only. Moreover, when there is multisynaptic bombardment of PSPs on the SIL (having a sufficient excess of excitation over inhibition), the process gives rise to a regular discharge pattern that reflects a correspondingly narrow distribution of first passage times. It may be of relevance that computer simulations show that, as the number of presynaptic terminals increase and the EPSP size decreases proportionately (so that the net excitation remains constant), the postsynaptic ISIs become more and more regular, regardless of the form of the presynaptic input process as long as there is independence between the input channels (Segundo et al., 1968).

Acknowledgements. We are very grateful for the substantial help provided by Messrs. A. D. Nicholas, B. E. Rodden, F. R. Wilson, V. Praestegaard, B. W. Lukey, R. P. S. Cardin, and L. A. Singer, and Doctors D. M. Sweeney and K. E. Money. This is DCIEM Research Paper 76-X-58. Some of the results reported herein were obtained during execution of a NASA contract NAS9-14641 (to M. J. Correia).

References

Bartlett, M.S.: Problemes de l'analyse spectral des series temporelles stationnaires. Publ. Inst. Statist., Univ. de Paris Fasc. **3**, 119—134 (1954)

Brassard, J.R., Correia, M.J., Landolt, J.P.: A computer program for the graphical and iterative fitting of probability density functions to biological data. Comp. Prog. Biomed. **5**, 11—38 (1975)

Calvin, W.H., Stevens, C.F.: Synaptic noise and other sources of randomness in motoneuron interspike intervals. J. Neurophysiol. **31**, 574—587 (1968)

Correia, M.J., Landolt, J.P.: Spontaneous and driven responses from primary neurons of the anterior semicircular canal of the pigeon. Fortschr. Hals.-Nas.-Ohrenheilk. **19**, 134—148 (1973)

Correia, M.J., Landolt, J.P., Cardin, R.P.S., Anderson, P.J., Lee, M. A.: Techniques for prolonged single unit recording and data analysis of discharges from primary neurons in the pigeon's vestibular ganglion, Report 927. Downsview, Ontario: Defence and Civil Institute of Environmental Medicine 1973

Cox, D.R., Lewis, P.A.W.: The statistical analysis of series of events. London: Methuen 1966

Cox, D.R., Miller, H.D.: The theory of stochastic processes. London: Methuen 1965

Detwiler, P.B., Fuortes, M.G.F.: Responses of hair cells in the statocyst of *Hermissenda*. J. Physiol. (Lond.) **251**, 107—129 (1975)

Engström, H., Bergström, B., Ades, H.W.: Macula utriculi and macula sacculi in the squirrel monkey. In: Inner ear studies. Ades, H. W., Engström, H., eds. Acta oto-laryng. Suppl. **301**, 75—126 (1972)

Feller, W.: On the Kolmogorov-Smirnov limit theorems for empirical distributions. Ann. Math. Stat. **19**, 177—189 (1948)

Fienberg, S.E.: Stochastic models for single neuron firing trains: a survey. Biometrics **30**, 399—427 (1974)

Flock, Å.: Sensory transduction in hair cells. In: Handbook of sensory physiology, Vol. I, pp. 396—441. Lowenstein, W. R., ed. Berlin-Heidelberg-New York: Springer 1971

Flock, Å., Russell, I.J.: The post-synaptic action of efferent fibres in the lateral line organ of the burbot *Lota lota*. J. Physiol. (Lond.) **235**, 591—605 (1973a)

Flock, Å., Russell, I.: Efferent nerve fibres: Postsynaptic action on hair cells. Nature **243**, 89—91 (1973b)

Flock, Å., Russell, I.: Inhibition by efferent nerve fibres: action on hair cells and afferent synaptic transmission in the lateral line canal of the burbot *Lota lota*. J. Physiol. (Lond.) **257**, 45—62 (1976)

Friedmann, I., Bird, E.S.: Electron microscopic studies of the isolated fowl embryo otocyst in tissue culture. Rudimentary kinocilia, cup-shaped nerve endings and synaptic bars. J. Ultrastruct. Res. **20**, 356—365 (1967)

Furukawa, T., Ishii, Y.: Neurophysiological studies on hearing in goldfish. J. Neurophysiol. **30**, 1377—1403 (1967)

Furukawa, T., Ishii, Y., Matsuura, S.: Synaptic delay and time course of postsynaptic potentials at the junction between hair cells and eighth nerve fibers in the goldfish. Japan J. Physiol. **22**, 617—635 (1972)

Goldberg, J.M., Fernandez, C.: Physiology of peripheral neurons innervating semicircular canals of the squirrel monkey. III. Variations among units in their discharge properties. J. Neurophysiol. **34**, 676—684 (1971)

Hashimoto, T., Katsuki, Y., Yanagisawa, K.: Efferent system of lateral line organ of fish. Comp. Biochem. Physiol. **33**, 405—421 (1970)

Himmelblau, D.M.: Process analysis by statistical methods. New York: Wiley 1970

Ishii, Y., Matsuura, S., Furukawa, T.: Quantal nature of transmission at the synapse between hair cells and eighth nerve fibers. Japan J. Physiol. **21**, 79—89 (1971)

Iurato, S., Taidelli, G.: Relationships and structures of the so-called "much granulated nerve endings" in the crista ampullaris (as studied by means of serial sections). In: Proceedings of third european regional conference of electron microscopy, pp. 325—326. Titlbach, M., ed. Prague: Czechoslovak Academy of Sciences 1964

Jenkins, G. M., Watts, D. G.: Spectral analysis and its application. San Francisco: Holden-Day 1968

Jørgensen, J. M., Andersen, T.: On the structure of the avian maculae. Acta Zool. **54**, 121—131 (1973)

Junge, D., Moore, G. P.: Interspike-interval fluctuations in aplysia pacemaker neurons. Biophys. J. **6**, 411—434 (1966)

Klinke, R., Galley, N.: Efferent innervation of vestibular and auditory receptors. Physiol. Rev. **54**, 316—357 (1974)

Kiang, N. Y.-S., Watanabe, T., Thomas, E. C., Clark, L. F.: Discharge patterns of single fibers in the cat's auditory nerve. Cambridge: Massachusetts Institute of Technology Press 1965

Landolt, J. P., Correia, M. J.: Neuromathematical concepts of point process theory. IEE Trans. Biomed. Eng. In press (1977)

Lewis, P. A. W.: Distribution of the Anderson-Darling statistic. Ann. Math. Stat. **32**, 1118—1123 (1961)

Lewis, P. A. W.: Some results on tests for Poisson processes. Biometrika **52**, 67—77 (1965)

Lewis, P. A. W.: Recent results in the statistical analysis of univariate point processes. In: Stochastic point processes: statistical analysis, theory, and applications, pp. 1—54. Lewis, P. A. W., ed. New York: Wiley Interscience 1972

Lewis, P. A. W., Goodman, A. S.: The null distribution of the first three product-moment statistics for exponential, half-gamma and normal scores, Report RC 2255. Yorktown Heights NY: IBM T. J. Watson Research Center 1968

Lewis, P. A. W., Katcher, A. M., Weis, A. H.: SASE IV—An improved program for the statistical analysis of series of events, Report RC 2365. Yorktown Heights NY: IBM T. J. Watson Research Center 1969

Lifschitz, W. S.: Responses from first order neurons of the horizontal semicircular canal in the pigeon. Brain Res. **63**, 43—57 (1973)

Lowenstein, O.: Peripheral mechanisms of equilibrium. Brit. Med. Bull. **12**, 114—118 (1956)

Pearson, E. S., Hartley, H. O.: Biometrika tables for statisticians, Vol. 1. Cambridge: Cambridge University Press 1970

Perkel, D. H., Gerstein, G. L., Moore, G. P.: Neuronal spike trains and stochastic point processes. 1. The single spike train. Biophys. J. **7**, 391—418 (1967)

Segundo, J. P., Perkel, D. H., Wyman, H., Hegstad, H., Moore, G. P.: Input-output relations in computer-simulated nerve cells. Influence of the statistical properties, strength, number and interdependence of excitatory pre-synaptic terminals. Kybernetik **4**, 157—171 (1968)

Shiavi, R., Negin, M.: The effect of measurement errors on correlation estimates in spike-interval sequences. IEEE Trans. Biomed. Eng. BME-**20**, 374—378 (1973)

Smith, C. A., Rasmussen, G. L.: Nerve endings in the maculae and cristae of the chinchilla vestibule, with a special reference to the efferents. In: Third symposium on the role of the vestibular organs in space exploration. SP-152, pp. 183—201. Washington, D. C.: National Aeronautics and Space Administration 1968

Spoendlin, H.: Innervation densities of the cochlea, Acta oto-laryng. **73**, 235—248 (1972)

Valli, P., Taglietti, V., Casella, C. E., Rossi, M. L.: Proprietá funzionali delle diverse unitá recettrici nei canali semicircolari isolati di rana. Arch. Fisiol. **70**, 94—95 (1973)

Walsh, B. T., Miller, J. B., Gacek, R. R., Kiang, N. Y.-S.: Spontaneous activity in the eighth cranial nerve of the cat. Int. J. Neurosci. **3**, 221—236 (1972)

Wersäll, J.: Studies on the structure and innervation of the sensory epithelium of the cristae ampullares in the guinea pig. Acta oto-laryng. Suppl. **126**, 1—85 (1956)

Received: June 21, 1977

Dr. M. J. Correia
Departments of Otolaryngology,
Physiology and Biophysics
Unit 9A
John Sealy Hospital
(R-8) UTMB
Galveston, TX 77550, USA

Dr. J. P. Landolt
Defence and Civil Institute
of Environmental Medicine
1133 Sheppard Ave. W.
P. O. Box 2000
Downsview, Ontario
Canada M3M 3B9